Knot Homologies from Landau-Ginsburg Models

Miroslav Rapčák

CERN

with Mina Aganagic and Elise LePage

Berkeley String-Math Seminar, November 28, 2022

1. Introduction

1.1. Polynomial invariants

- We will be interested in a construction of various topological invariants associated to links in $\mathbb{R}^3$, such as the Hopf link

that we are going to use for illustration purposes.

- There exists a large zoo of polynomial invariants such as the famous Jones polynomial [Jones (1985)]

$$\chi_{Jones}(q) = q + q^{-1}.$$

- Its rescaled version is the $\mathfrak{gl}(2)$ invariant

$$\chi_{\mathfrak{gl}(2)}(q) = (q^{\frac{1}{2}} + q^{-\frac{1}{2}})\chi_{Jones}(q) = q^{3/2} + q^{1/2} + q^{-1/2} + q^{-3/2}.$$

- There also exist polynomial invariants associated to other Lie (super) algebras, in particular the series $\mathfrak{gl}(m|n)$.

1.2. Homological invariants

- Polynomial invariants often admit categorification in terms of homological invariants.
- An example is the Khovanov homology [Khovanov (2000)]

$$KH = \oplus_{i,j} KH^{i,j},$$

that is the homology of a complex

$$\cdots \to C^{0,*} \to C^{1,*} \to C^{2,*} \to \dots$$

associated to a link.

- The $\mathfrak{gl}(2)$ invariant can be recovered as the Euler characteristic of the complex:

$$\chi(q) = \sum_{i,j} (-1)^i \dim(KH^{i,j}) q^j.$$

- People have also constructed homological invariants associated to $\mathfrak{gl}(m)$ and $\mathfrak{gl}(1|1)$ (aka Heegaard-Floer-knot homology).

- For example, the complex for the Hopf link reads

$$
\begin{matrix} \mathbb{C}^{0,\frac{1}{2}} \\ \mathbb{C}^{0,-\frac{1}{2}} \\ \mathbb{C}^{0,-\frac{1}{2}} \\ \mathbb{C}^{0,-\frac{3}{2}} \end{matrix}
\xrightarrow{\begin{pmatrix} 1 & 0 & 0 & 0 \\ 1 & 0 & 0 & 0 \\ 0 & 1 & 1 & 0 \\ 0 & 1 & 1 & 0 \end{pmatrix}}
\begin{matrix} \mathbb{C}^{1,\frac{1}{2}} \\ \mathbb{C}^{1,\frac{1}{2}} \\ \mathbb{C}^{1,-\frac{1}{2}} \\ \mathbb{C}^{1,-\frac{1}{2}} \end{matrix}
\xrightarrow{\begin{pmatrix} 0 & 0 & 0 & 0 \\ 1 & -1 & 0 & 0 \\ 1 & -1 & 0 & 0 \\ 0 & 0 & -1 & 1 \end{pmatrix}}
\begin{matrix} \mathbb{C}^{2,\frac{3}{2}} \\ \mathbb{C}^{2,\frac{1}{2}} \\ \mathbb{C}^{2,\frac{1}{2}} \\ \mathbb{C}^{2,-\frac{1}{2}} \end{matrix}
$$

- The homology is four-dimensional, concentrated at degrees

$$KH^{2,\frac{3}{2}} = KH^{2,\frac{1}{2}} = KH^{0,-\frac{1}{2}} = KH^{0,-\frac{3}{2}} = \mathbb{C}.$$

- We obviously recover the $\mathfrak{gl}(2)$ invariant as

$$
\begin{aligned}
\chi(q) &= (-1)^2 q^{\frac{3}{2}} + (-1)^2 q^{\frac{1}{2}} + (-1)^0 q^{-\frac{1}{2}} + (-1)^0 q^{-\frac{3}{2}} \\
&= q^{\frac{3}{2}} + q^{\frac{1}{2}} + q^{-\frac{1}{2}} + q^{-\frac{3}{2}}.
\end{aligned}
$$

1.3. Physical/geometric origin

- Polynomial invariants are known to originate from $\mathfrak{gl}(m|n)$ Chern-Simons theory in terms of the expectation value of line operators [Witten (1989)].
- But what is the physics behind homological invariants? Can one reproduce the success of the Chern-Simons theory and learn something new about them?
- An attempt to find such a physical story was presented by [Witten (2011)] and later developed by multiple other people but its complicated nature does not allow any non-trivial calculations.
- Utilising various string-theory dualities and building up on the insights from the work of [Ozscath-Szabo (2008), Auroux (2010), Rasmussen (2003), Seidel-Smith (2008), Gaiotto-Moore-Witten (2015), Webster (2015), . . .], Mina Aganagic proposed a new framework to compute the $\mathfrak{gl}(2)$ invariant of links [Aganagic (2020), (2021), (2022)].

1.4. Plan for today:

- Review some aspects of the Aganagic's proposal.
- Turn it into a calculational tool by making the problem algebraic. [Aganagic-LePage-MR (very soon)]
- Sketch the proof of topological invariance. [Aganagic-LePage-MR (very soon)]
- Comment on the generalization to $\mathfrak{gl}(m|n)$ homological invariants. For $\mathfrak{gl}(1|1)$, see [Aganagic-LePage-MR (very soon)] and for $\mathfrak{gl}(m|n)$, see [Aganagic-LePage-MR (soonish)].

2. Aganagic's proposal

2.1. Overview

- Aganagic proposes 4 physical pictures that lead to link invariants. They are mutually related by mirror symmetry in a combination with equivariant localization.
- Today, we are going to be interested in one of the constructions based on the Landau-Ginsburg model living on the strip $\mathbb{R} \times I$ with the target being an n'th symmetric power of a punctured Riemann surface.
- KH can be then identified with the space of supersymmetric groundstates of this model for a particular choice of boundary conditions on the two sides of I.
- As promised above, we are going to illustrate the whole construction on the example of the Hopf link:

2.2. Stretching the knot

- Let us start with a knot in $\mathbb{R}^3$, stretch it along one direction as

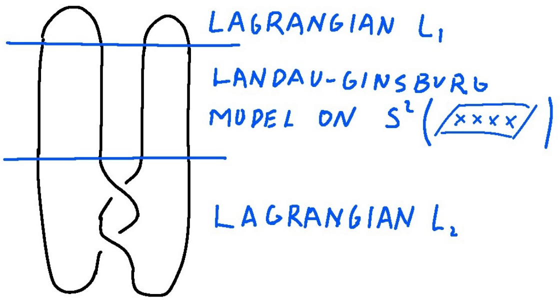

and cut it into three pieces as show in the figure.

2.3. What target?

- The middle slice of

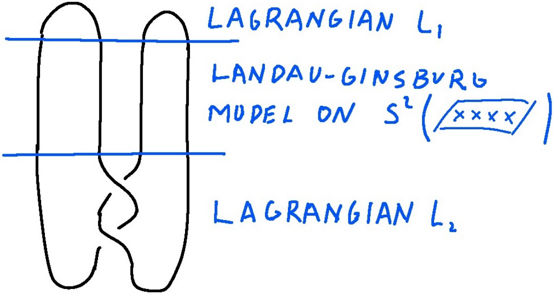

has the geometry of $\mathbb{C} \times I$ with knot bits inserted along I and placed at fixed positions $z_1, \ldots z_{2n} \in \mathbb{C}$. Let us denote the resulting punctured plane by Σ.

- The desired target space is then $X = \mathrm{Sym}^n \, \Sigma$ and in our Hopf-link example, the second symmetric power of a four-punctured plane.

2.3. What potential?

- The potential $W(x_1, \ldots, x_n)$ is a function on $\mathrm{Sym}^n\, \Sigma$ and a natural source of such functions associated to Lie algebras are conformal blocks.
- For example, conformal blocks of the Virasoro algebra $\mathcal{W}_2$ on a plane with an insertion of $2n$ vertex operators in the fundamental representation at z_i can be written as

$$\oint_C dx_1 \ldots dx_n \prod_{i<j} (z_i - z_j)^{-\epsilon} \prod_{i \neq j} (x_i - x_j)^{-\epsilon} \prod_{i,j} (x_i - z_j)^{\epsilon}$$

where different choices of the contour C parametrize different conformal blocks. [Dotsenko-Fateev (1984), Felder (1989)]

- The desired potential W encoding the equivariant grading together with the holomorphic form Ω encoding the Maslov grading can be read off from the integrand of the above expression by

$$\Omega e^{\epsilon W} \quad = \quad dx_1 \dots dx_n \prod_{i \neq j} (x_i - x_j)^{-\epsilon} \prod_{i,j} (x_i - z_j)^{\epsilon}$$

  where $z_1, \dots, z_{2n}$ are positions of our knot strands and $x_1, \dots, x_n$ are coordinates on $\mathrm{Sym}^n \Sigma$. We have also dropped x_i-independent terms since they only contribute by a constant shift to the potential.
- Concretely, we have

$$\Omega = dx_1 \dots dx_n, \quad W = -\sum_{i \neq j} \log(x_i - x_j) + \sum_{i,j} \log(x_i - z_j)$$

- The choice of the contour C is going to be related to the choice of boundary conditions for our model as we are going to see next.

2.4. Caps

- We have associated the Landau-Ginsburg model on $I \times \mathbb{R}$ to the middle slice. From the perspective of this middle part, the other two slices specify a boundary condition on the two sides of the interval I.
- To a collection of caps, we associate a Lagrangian that is a symmetric product of lines in Σ stretched between two punctures joined by an arch.
- In our example

2.4. Cups

- If the knot strands on the other side had been simple cups, the Lagrangians would have been symmetric products of figure eights:

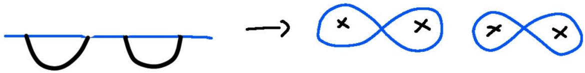

- But since they are more complicated, we need to braid them

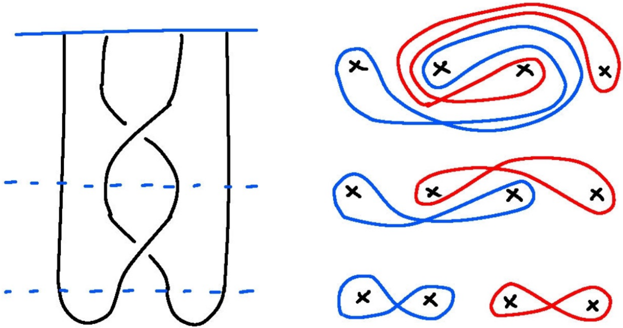

2.5. Intersection points

- Desired homological invariants arise from counting intersection points between the cap Lagrangian L_1 and the braided cup Lagrangian L_2 in our Landau-Ginsburg model.
- The analogue of the Khovanov's homological degree is the standard Maslov degree encoded by Ω. The analogue of the ϵ degree is the equivariant degree encoded by W. These come from the lift of the phase of $\Omega e^{\epsilon W}$ into a single-valued function on L_1 and L_2.
- Can we find an algorithm to find these intersection points in possibly complicated configurations?
- We are going to find a solution to this problem by making the problem algebraic.

3. Single strand $n = 1$

3.1. The boring unknot

- At first sight, the configuration containing a single pair of punctures seems boring since

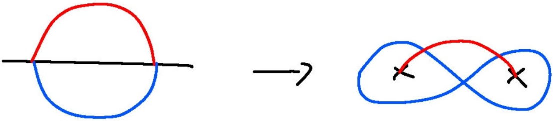

corresponding to the unknot would be the only configuration one can engineer.

3.2. Reduced homology

- Luckily, it turns out that cutting one of the strands such as in

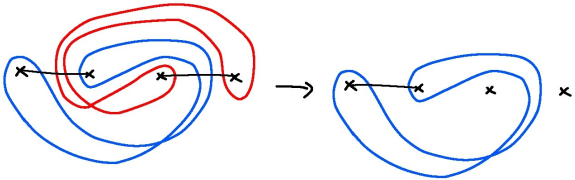

leads to the reduced-homology invariant categorifying

$$\chi_{Jones}(q) = \frac{\chi_{\mathfrak{gl}(2)}(q)}{q^{1/2} + q^{-1/2}}.$$

- Using this proposal, finding reduced homology for any rational knot (those coming from capping a braid of four strands) becomes almost trivial.

3.3. Intersection points

- In this simple example, we can immediately see that there are two intersection points and there is no disk not intersecting with a puncture that could possibly lead to a non-trivial differential:

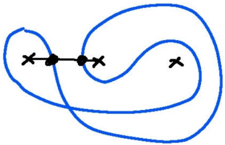

- Identifying degrees of the punctured disk allows us to identify their relative Maslov and equivariant degrees and then recover the Jones polynomial $q + q^{-1}$.
- Counting disks in more complicated setups (more involved braiding and multiple strands) becomes a rather involved problem, so we will now develop an algebraic approach.

3.4. Thimbles

- Each brane in our category of branes can be represented in terms of a complex of a special set of (thimble) branes T_i generating our brane category (projective generators).
- Thimbles T_i are branes supported along straight lines in between punctures such as the five thimbles in

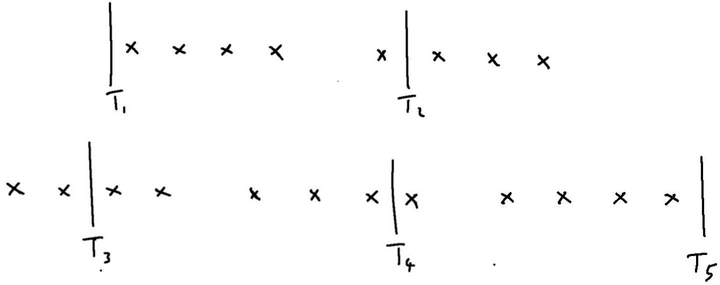

3.5. Morphisms between thimbles

- Morphisms between branes are in correspondence with their intersection points.
- Naively, thimbles do not intersect but deforming one of the branes (tilting in our picture), one can identify non-trivial morphisms. In particular, we find one morphism $T_i \to T_j$ for each pair T_i, T_j:

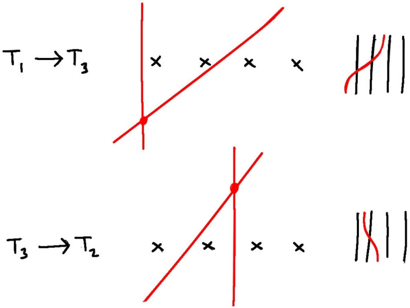

- We are going to use a strand notation for the morphisms.

3.6. Adding dots and the KLRW algebra

- Branes in Landau-Ginsburg models can generally carry more structure since they can support a nontrivial flat vector bundle. To get the desired invariant, we need to introduce such a modification resulting into the algebra of strands decorated by dots

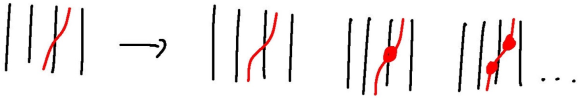

- This algebra is known as the KLRW algebra [Webster (2019), Aganagic-Danilenko-Li-Zhou (in progress)] and was previously studied from a dual B-model perspective.

3.7. Composing morphisms

- The algebra structure can be determined by identifying disks.
- For example, let us start with $T_2 \to T_3$:

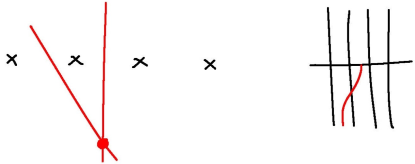

and compose with $T_3 \to T_4$:

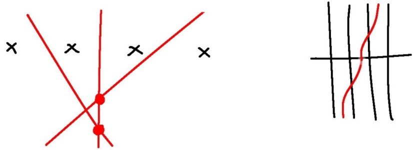

- The existence of the Maslov-degree-zero disk

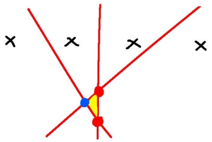

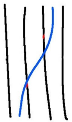

  tells us that the composition is non-trivial and allows us to identify the product in terms of the morphism associated with the blue intersection point.

- The resulting algebra is given by composition of strands together with relation

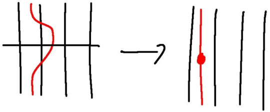

  when the two strands go in opposite directions [Webster (2022), Aganagic-Danilenko-Peng (in progress)].

3.8. Grading

- Looking at the potential and identifying the ϵ degree of various disks, one can show that assigning degrees

gives a consistent grading on the strand algebra.

3.9. Resolving brane

- We have found that the algebra of $\mathrm{Hom}(T, T)$ for $T = \bigoplus_i T_i$ admits a nice description in terms of the above strand algebra. We are now going to use T to describe a Lagrangian L in terms of a complex of thimbles T_i.
- First, one can construct a module for the strand algebra $\mathrm{Hom}(T, T)$ by intersecting the Lagrangian L with T, i.e. identifying $\mathrm{Hom}(T, L)$.
- Secondly, finding a projective resolution of such a module yields the desired complex of thimbles.
- This is a rather non-trivial construction and we are going to find an alternative proposal.

3.10. Resolving brane - an alternative proposal

- We would like to represent the brane of interest as a complex of thimbles T_i with the differential given by a collection of strand-algebra elements.
- It turns out that in the simple example of a single strand, we can read off the complex almost completely directly from the geometry!
- This is rather surprising since finding a projective resolution explicitly is usually a rather challenging task.
- In the first step, let us stretch our cycle into vertical bits resembling thimbles and horisontal bits corresponding to maps between them:

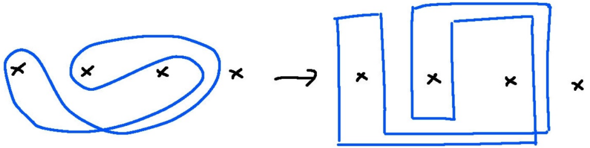

- Using the stretched representation of the cycle

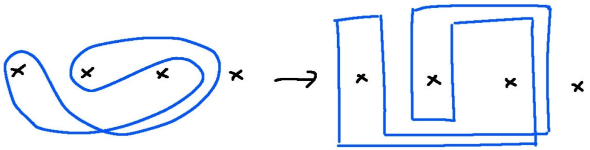

one can read off directly:

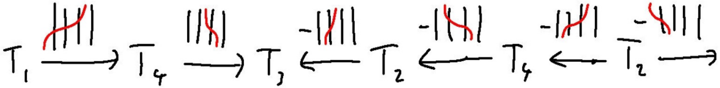

- Colapsing the above into a standard complex produces

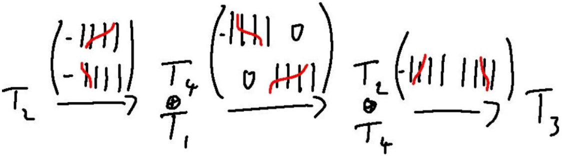

- This complex closes only up to dotted generators.
- One can easily find the full complex by writing an ansatz for all possible dotted corrections consistent with the equivariant and the Maslov degree and solve for $\delta^2 = 0$. One gets

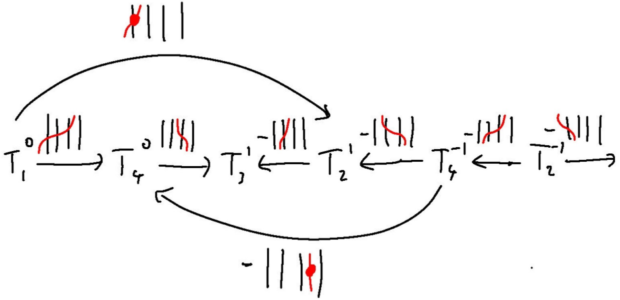

- More importantly, one can assign the ϵ degree to all thimbles by knowing the degree of our strand-algebra generators.

3.11. Reduced homology

- To find the reduced homology, we need to intersect with the cap brane.
- One can see that the I_i brane stretched between the $(i-1)$'th and i'th puncture has a one-dimensional intersection only with T_i, i.e. $\mathrm{Hom}(T_i, I_j) = \mathbb{C}\delta_{i,j}$:

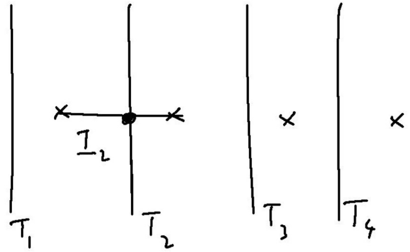

- Intersecting with I_2 thus picks all the T_2 factors in our complex.

- In our example

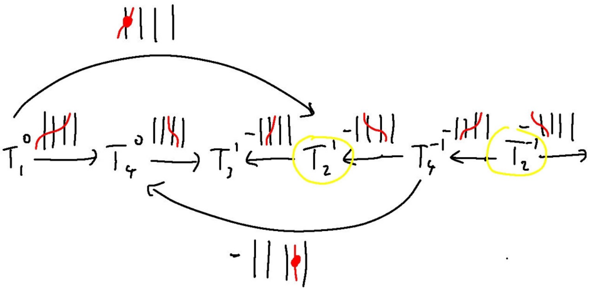

and we indeed get a two-dimensional homology

$$H^4 = \mathbb{C}\{1\}, \qquad H^2 = \mathbb{C}\{-1\}$$

with the Euler characteristic recovering the Jones polynomial

$$\chi = (-1)^4 q^1 + (-1)^2 q^{-1} = q + q^{-1}$$

4. Multiple strands $n > 1$

4.1. General stategy

- Working on symmetric products is much more challenging.
- Intersection points become n-touples of points on the punctured surface and one has nontrivial disks such as

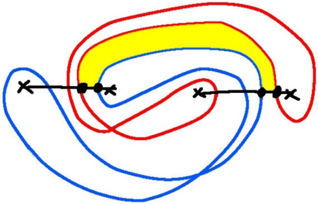

  These are hard to count.
- We are going to solve the problem by
  1. Taking a naive symmetric product of the individual complexes we found above.
  2. Writing an ansatz for correction terms in the differential δ and solving for $\delta^2 = 0$. This step makes counting disks algebraic!

4.2. Strand algebra

- Thimbles are now symmetric products of thimbles T_i from before. For example, for $n = 2$, we have a thimble

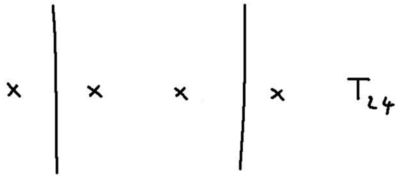

- Morphisms are going to be represented by n strands. Note that we have multiple intersection points between each pair of thimbles and correspondingly, we have strands that do or do not cross. For example

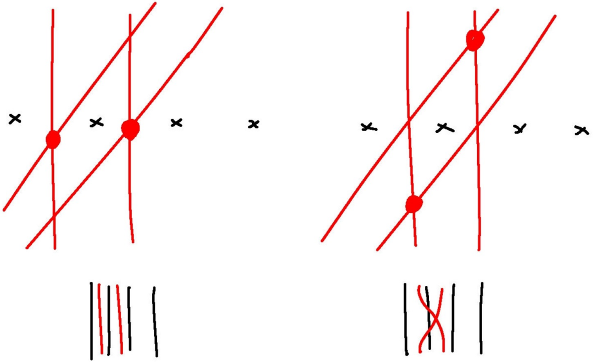

- Analogously to the single-strand case, one can analyze Maslov-degree-zero disks and derive all the relations in the strand algebra.
- Disks now look more complicated such as the one in

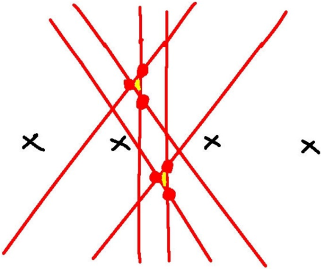

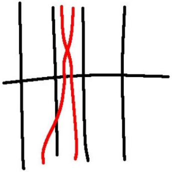

- The full set of relations in the upstairs algebra consists of the above relations from the $n = 1$ case together with

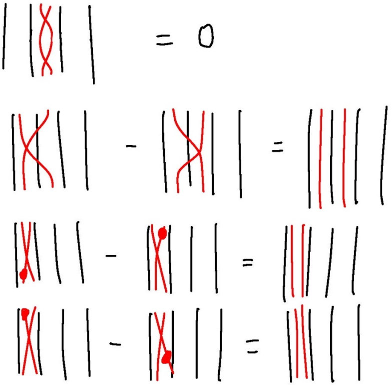

- This defines the full KLRW algebra. [Webster (2015)]

4.3. Resolving individual cycles

- Recall that we can resolve individual cycles of

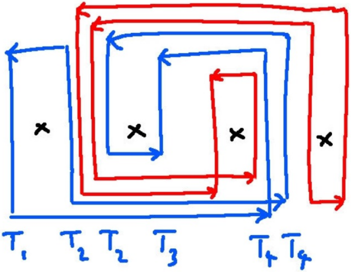

(up to dotted corrections) as

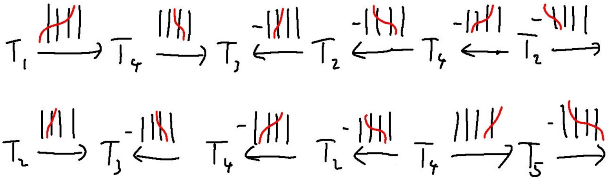

4.4. Taking naive product

- The naive symmetric product produces a grid of thimbles

$$
\begin{tikzcd}
 & T_2 \arrow[r] & T_3 & T_4 \arrow[l] & T_2 \arrow[l] & T_4 \arrow[l] \arrow[r] & T_5 \arrow[r] & {} \\
T_1 \arrow[d] & T_{12} \arrow[r] \arrow[d] & T_{13} \arrow[d] & T_{14} \arrow[l] \arrow[d] & T_{12} \arrow[l] \arrow[d] & T_{14} \arrow[l] \arrow[r] \arrow[d] & T_{15} \arrow[d] & \\
T_4 \arrow[d] & T_{24} \arrow[r] \arrow[d] & T_{34} \arrow[d] & T_{44} \arrow[l] \arrow[d] & T_{24} \arrow[l] \arrow[d] & T_{44} \arrow[l] \arrow[r] \arrow[d] & T_{45} \arrow[d] & \\
T_3 & T_{23} \arrow[r] & T_{33} & T_{34} \arrow[l] & T_{23} \arrow[l] & T_{34} \arrow[l] \arrow[r] & T_{35} & \\
T_2 \arrow[u] & T_{22} \arrow[r] \arrow[u] & T_{23} \arrow[u] & T_{24} \arrow[l] \arrow[u] & T_{22} \arrow[l] \arrow[u] & T_{24} \arrow[l] \arrow[r] \arrow[u] & T_{25} \arrow[u] & \\
T_4 \arrow[u] & T_{24} \arrow[r] \arrow[u] & T_{34} \arrow[u] & T_{44} \arrow[l] \arrow[u] & T_{24} \arrow[l] \arrow[u] & T_{44} \arrow[l] \arrow[r] \arrow[u] & T_{45} \arrow[u] & \\
T_2 \arrow[u] \arrow[d] & T_{22} \arrow[r] \arrow[u] \arrow[d] & T_{23} \arrow[u] \arrow[d] & T_{24} \arrow[l] \arrow[u] \arrow[d] & T_{22} \arrow[l] \arrow[u] \arrow[d] & T_{24} \arrow[l] \arrow[r] \arrow[u] \arrow[d] & T_{25} \arrow[u] \arrow[d] & \\
{} & {} & {} & {} & {} & {} & {} &
\end{tikzcd}
$$

- The crossing/straight strands can be identified directly from the picture

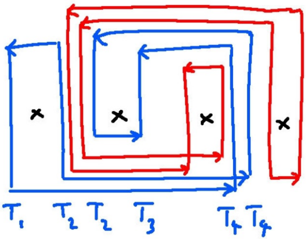

by identifying if the given morphism line crosses the second thimble as in

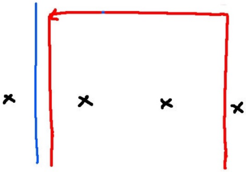

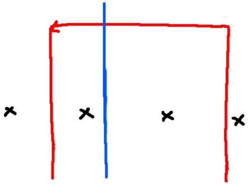

- One can collapse the above grid of maps into a standard complex of the form

$$
T_{24}^{-4} \longrightarrow
\begin{array}{c} T_{44}^{-4} \\ T_{25}^{-4} \\ T_{14}^{-3} \\ T_{22}^{-2} \end{array}
\longrightarrow
\begin{array}{c} T_{45}^{-4} \\ T_{15}^{-3} \\ T_{44}^{-3} \\ T_{24}^{-3} \\ T_{24}^{-2} \\ T_{24}^{-2} \\ T_{12}^{-1} \\ T_{22}^{-1} \end{array}
\longrightarrow
\begin{array}{c} T_{45}^{-3} \\ T_{44}^{-3} \\ T_{24}^{-2} \\ T_{34}^{-2} \\ T_{25}^{-2} \\ T_{24}^{-2} \\ T_{14}^{-1} \\ T_{22}^{-1} \\ T_{23}^{-1} \\ T_{12}^{0} \end{array}
\longrightarrow
\begin{array}{c} T_{44}^{-2} \\ T_{35}^{-2} \\ T_{24}^{-2} \\ T_{34}^{-2} \\ T_{24}^{-1} \\ T_{23}^{-1} \\ T_{13}^{0} \\ T_{22}^{0} \end{array}
\longrightarrow
\begin{array}{c} T_{34}^{-2} \\ T_{34}^{-1} \\ T_{23}^{-1} \\ T_{23}^{0} \end{array}
\longrightarrow T_{33}^{-1}
$$

and assign the ϵ grading to each of the thimble.

- The first two differentials are explicitly

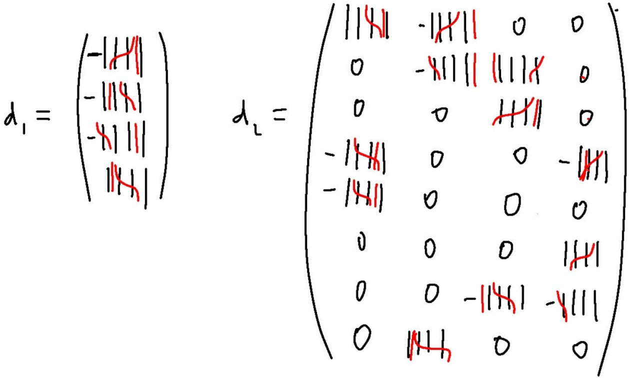

and analogously for d_3, d_4, d_5, d_6.

4.5. Adding dots

- One can decorate the complex by adding dotted corrections:

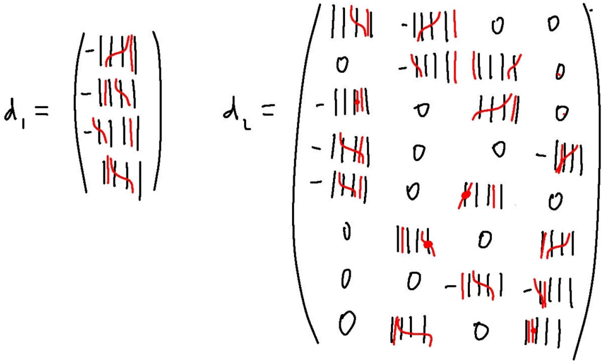

4.6. Ansatz for corrected differential

- To "count disks algebraically", let us write an asatz for correction terms in the differential by including all maps consistent with the Maslov and the ϵ grading and that do not contain any dots:

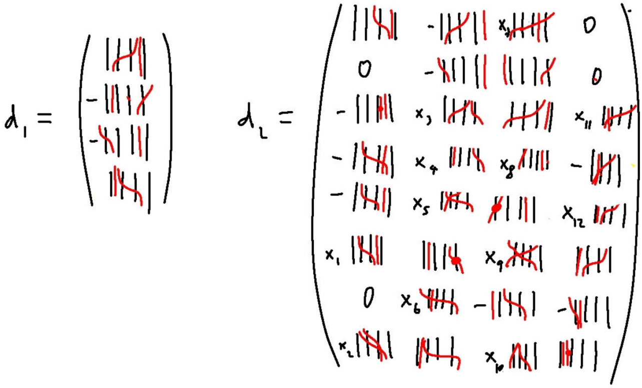

4.7. Solving for $\delta^2 = 0$

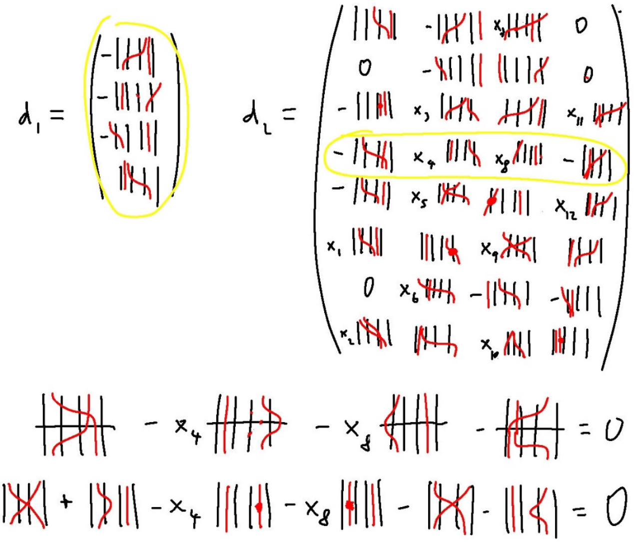

$\Rightarrow \quad x_4 = x_8 = -1$

- The full solution reads

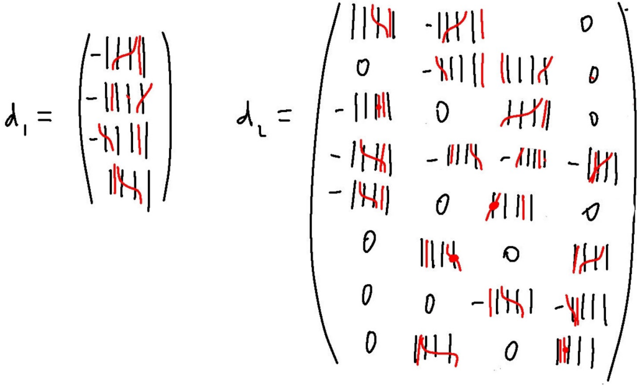

4.9. Intersecting with caps

- Intersecting with the cap brane I_{24} selects

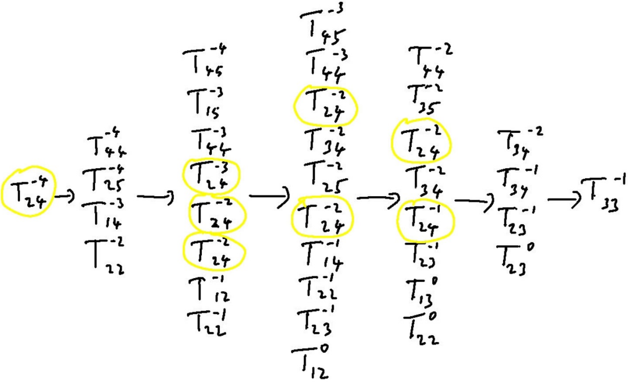

- The resulting complex reads

$$\begin{matrix}\mathbb{C}\{-2\}\\ \oplus \\ \mathbb{C}\{-1\}\end{matrix} \xrightarrow{\begin{pmatrix}-1 & 0\\ -1 & 0\end{pmatrix}} \begin{matrix}\mathbb{C}\{-2\}\\ \oplus \\ \mathbb{C}\{-2\}\end{matrix} \xrightarrow{\begin{pmatrix}0 & 0\\ 1 & -1\\ -1 & 1\end{pmatrix}} \begin{matrix}\mathbb{C}\{-3\}\\ \oplus \\ \mathbb{C}\{-2\}\\ \oplus \\ \mathbb{C}\{-2\}\end{matrix} \longrightarrow \phi \longrightarrow \mathbb{C}\{-4\}$$

- The homology is given by

$$H^0 = \mathbb{C}\{-1\}, \qquad H^2 = \mathbb{C}\{-3\} \oplus \mathbb{C}\{-2\}, \qquad H^4 = \mathbb{C}\{-4\}$$

- One recovers the $\mathfrak{gl}(2)$ invariant (up to the overall factor) as the Euler characteristic

$$\begin{aligned}\chi &= (-1)^0 q^{-4} + (-1)^2(q^{-3} + q^{-2}) + (-1)^4 q^{-1}\\ &= q^{-5/2}(q^{3/2} + q^{1/2} + q^{-1/2} + q^{-3/2})\end{aligned}$$

- We have checked the construction for all knots up to seven crossings! . . . Using computer. . .

6. Topological invariance

6.1. Topological invariance

- To show topological invariance, one needs to check multiple moves [Bigelow (2002)].
- The following three

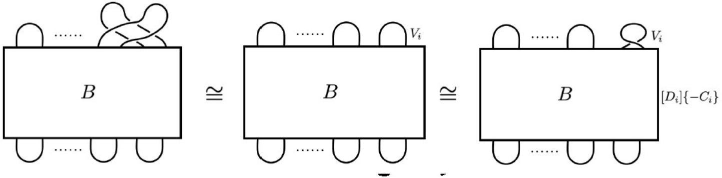

are obviously satisfied by construction.

- On the other hand, the other two moves are

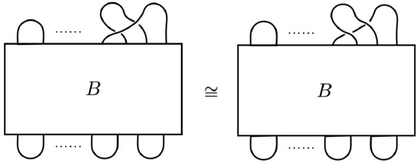

and

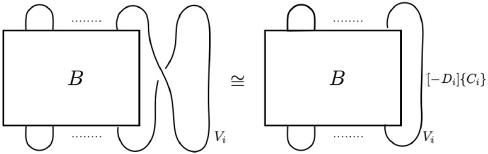

- They translate into the equivalence of

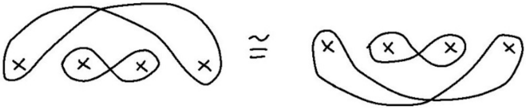

and

- Both transitions are implied by a simpler move

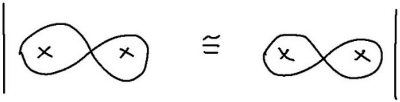

6.2. Sketch of the proof

- To prove the equivalence, we can first resolve the branes L_1 and L_2 on each side in terms of complexes of thimbles.
- Identify chain maps $f_1 : L_1 \to L_2$ and $f_2 : L_2 \to L_1$ so that both $f_1 \circ f_2$ and $f_2 \circ f_1$ are homotopic to the identity morphism.
- This can be shown by an explicit calculation.

6. Generalization to $\mathfrak{gl}(k|l)$

6.1. Target space

- For general $\mathfrak{gl}(k|l)$, the target space consists of $k+l-1$ copies of the above symmetric power

$$X = (\mathrm{Sym}^n \Sigma)^{k+l-1}$$

(one for each simple root).

- We are going to call each factor corresponding to the fermionic root fermionic.

6.2. Potential

- To find the potential, realize an existence of a two-parametric generalization of the Virasoro algebra $\mathcal{W}_{k|l}$ [Gaiotto-MR (2017)] that generalizes further the well-known $\mathcal{W}_k$ algebra known e.g. from the AGT correspondence.
- Analogously to the Virasoro algebra $\mathcal{W}_2$ above, one can write down conformal blocks with the insertion of fundamental and anti-fundamental vertex operators in the free-field realization [Prochazka-MR (2018)].
- The integrand can be again identified with $\Omega e^{\epsilon W}$ of our Landau-Ginsburg model that allows us to identify the Maslov and the equivariant degree. Note that in the free-field realization, we are required to introduce $k+l-1$ screening currents for each simple root.

6.2. Potential

- Compared to the $\mathfrak{gl}(2)$ case, we need to distinguish the fundamental and the anti-fundamental representation (decoupling the diagonal $\mathfrak{gl}(1)$ factor, they were indistinguishable). We need n insertions of the fundamental and n insertions of the anti-fundamental field.
- Note that Ω can generally receive further contributions compared to the above if the integrand contains ϵ-independent factors.
- Note also the non-trivial duality

$$k \leftrightarrow l \qquad \epsilon \leftrightarrow -1-\epsilon$$

  This gives an alternative grading even in the $\mathfrak{gl}(2)$ story above.

6.3. Branes

- We are going exchange a single figure-eight by a bundle of figure-eights for each bosonic root and ovals for each fermionic root.
- For example, a cup in the $\mathfrak{gl}(2|1)$ invariant is going to be represented by

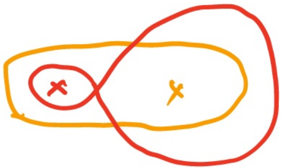

6.4. Strand algebra

- The strand algebra consists of strands of different colors.
- First, we need to distinguish fundamental and anti-fundamental punctures.
- Secondly, each strand is labelled by the corresponding simple root.
- Fermionic roots do not support any dots.
- Counting disks, one can easily derive relations in the strand algebra. They are analogous but more complicated to write down.
- From the potential, one can easily derive the Maslov and the equivariant degree.
- One substantial difference is that for $m \neq 0 \neq n$, there is a non-trivial differential Q turning the strand-algebra into a differential-graded-algebra.

6.5. Counting disks

- To count disks algebraicaly, one needs to first write the approximate differential δ_0 analogously to the above. (There is one technical complication requiring us to remove some of the geometric maps.)
- For super-algebras, some of the geometric maps do not have Maslov degree one and we need to introduce twisted complexes with an approximate differential δ_0.
- To find the deformation $\delta = \delta_0 + \delta_1$, we need to solve the Maurer-Cartan equation

$$Q\delta + \delta^2 = 0$$

7. Summary

- We have developed a new algorithm for computing the Khovanov homology and the $\mathfrak{gl}(1|1)$ homology (aka Heegaard-Floer-knot homology).
- We have a proposal for invariants associated to any $\mathfrak{gl}(k|l)$ and more. More checks are being done.